Comparison between the many-body perturbative and Green's-function approaches for calculating electron binding energies and affinities: Brueckner and Dyson orbitals

Ingvar Lindgren

November 30, 2003

Abstract. The many-body perturbative and Green's-function approaches for evaluating electron binding energies and electron affinities are compared, and it is shown that they are equivalent and both virtually exact. The former approach leads to Brueckner orbitals and the latter to Dyson orbitals, and it is shown that the two concepts are identical for a single valence electron or valence hole. The eigenvalue yields the exact binding energy/affinity, including correlation and relaxation effects. This result can be shown to hold also under more general conditions.

Keywords: Many-body perturbation theory, Green's-function technique, Brueckner orbital, Dyson equation, Dyson orbital, self energy, electron affinity

Table of Contents

1. Introduction

The electron binding energy or removal energy represents the energy needed to remove an electron from an electronic system and is given by the energy difference between the final and initial states of the process. There exist today a number of more or less sophisticated methods for evaluating this quantity. In the Hartree-Fock method, the orbital energy eigenvalue is according to Koopmans' theorem [21] equal to the corresponding removal energy (with opposite sign), if the remaining orbitals are assumed to be *frozen*. This implies that the effect of *'relaxation'* is neglected – an effect which for inner-shell ionization can be quite appreciable. A simple and popular way of including the relaxation effect in an approximate way is to perform separate self-consistent-field calculations of the system before and after the ionization – a technique commonly known as the ΔSCF *method*. In this technique also approximate methods with local exchange can be used without any noticeable loss of accuracy. This technique has been frequently used since the 1960's for atoms and somewhat later for molecules.

Since the Koopmans and the ΔSCF techniques are based upon the single-particle picture, true many-body effects are not included. These effects can be handled by means of *many-body perturbation theory* (MBPT) [26] or by means of the *Green's-function technique* (GF) [33], and particularly the latter method is now frequently used in quantum chemistry.

Treating the ionization process by means of MBPT, leads to *Brueckner orbitals* or *maximum-overlap orbitals* [7, 32, 25], while the GF technique leads to what is now known as *Dyson orbitals* [8, 20]. It has been known for quite some time that the Brueckner orbitals leads to the correct binding energy [26, 31, 28], which is also the case for the Dyson orbital [13]. Nevertheless, there has been some confusion lately in the quantum-chemistry community about the relation between these techniques and to what extent they are equivalent. In the present work the two techniques will be compared and *it is shown that for a single electron outside closed shells – or a single hole in closed shells – the concepts of Brueckner and Dyson orbitals are identical*. It can be shown that this is true also under more general conditions, as will be discussed in a forthcoming publication.

During recent years amazingly accurate electron binding energies have also been evaluated for atoms as well as complex molecules by means of *density-functional theory* (DFT) [9, 42], but we shall not be concerned with this technique here.

In the next section we shall summarize the many-body perturbation theory (MBPT) and its graphical representation (for further details,

see, for instance, ref. [26]). Those who are familiar with these concepts can go directly to Section 3.

2. Many-body perturbation theory

2.1. The Bloch equation

We are interested in solving the Schrödinger equation for a number of states of an N-electron system

$$H\Psi^\alpha = E^\alpha \Psi^\alpha \qquad (\alpha = 1, 2, \dots d), \tag{1}$$

known as the *target states*. The Hamiltonian is (in atomic units, $e = m = \hbar = 4\pi\epsilon_0 = 1$)

$$H = \sum_{i=1}^{N} \Big(-\frac{1}{2}\nabla_i^2 + v_{\rm ext}(\boldsymbol{x}_i)\Big) + \sum_{i<j}^{N} \frac{1}{r_{ij}}, \tag{2}$$

where $-\frac{1}{2}\nabla^2$ represents the kinetic energy, $v_{\rm ext}(\boldsymbol{x})$ the external (nuclear) potential and $1/r_{ij}$ the interelectronic interaction.

The Hamiltonian is partitioned in the standard way into a zeroth-order Hamiltonian and a perturbation

$$H = H_0 + H'. \tag{3}$$

The zeroth-order Hamiltonian is supposed to be of single-particle type

$$H_0 = \sum_{i}^{N} h_0(i) = \sum_{i}^{N} \Big(-\frac{1}{2}\nabla_i^2 + v_{\rm ext}(\boldsymbol{x}_i) + u_i\Big), \tag{4}$$

and the perturbation is then

$$H' = -\sum_{i}^{N} u_i + \sum_{i<j}^{N} \frac{1}{r_{ij}}\,. \tag{5}$$

Here, u_i is an optional potential, which can be a local function or a nonlocal potential, such as the Hartree-Fock potential.

The single-electron orbitals are eigenfunctions of h_0

$$h_0\,\phi_i(\boldsymbol{x}) = \varepsilon_i\,\phi_i(\boldsymbol{x}), \tag{6}$$

and the Slater determinants ($\{\Phi_K\}$) composed of these orbitals form the basis of our calculation. These are eigenfunctions of H_0

$$H_0\,\Phi_K = E_0^K\,\Phi_K \tag{7}$$

with the eigenvalue equal to the sum of the eigenvalues of the occupied orbitals

$$E_0^K = \sum_i^{\text{occ}} \varepsilon_i. \tag{8}$$

For each of the target states there exist a *model state*, Ψ_0^α, confined to a functional subspace of eigenfunctions of H_0, known as the *model space* (P). We define a *wave operator* in such a way that it transforms each model function to the corresponding exact wave function

$$\Psi^\alpha = \Omega\, \Psi_0^\alpha \qquad (\alpha = 1, 2, \dots d). \tag{9}$$

We employ *intermediate normalization*, $\langle \Psi^\alpha | \Psi_0^\alpha \rangle = 1$, which implies that

$$P\Omega P = P, \tag{10}$$

where P is the projection operator for the model space. All states that are degenerate with a model state and that can be mixed with that state by the perturbation must be included in the model space.

Operating on the Schrödinger equation (1) by P from the left yields

$$H_{\text{eff}} \Psi_0^\alpha = E^\alpha \Psi_0^\alpha, \tag{11}$$

where

$$H_{\text{eff}} = PH\Omega P \tag{12}$$

is the *effective Hamiltonian*. Thus, *the model functions* (9) *are eigenfunctions of the effective Hamiltonian with the eigenvalues being the corresponding exact energies*.

The wave operator satisfies the *Bloch equation* [4, 3, 23, 29, 26]

$$\big[\Omega, H_0\big] P = \big(H'\Omega - \Omega W\big) P. \tag{13}$$

Here, the model space need not be degenerate. W is referred to as the *effective interaction* and in intermediate normalization given by

$$W = PH'\Omega P. \tag{14}$$

By expanding the wave operator perturbatively

$$\Omega = 1 + \Omega^{(1)} + \Omega^{(1)} + \cdots \tag{15}$$

a *generalized Rayleigh-Schrödinger perturbation expansion* can directly be generated from the Bloch equation [29, 26]. Then by diagonalizing the matrix of H_{eff} (12), the model functions and the energy of the target states are obtained to the corresponding accuracy, and the target functions can be constructed.

2.2. Second quantization and the particle-hole formalism

Instead of an order-by-order expansion of the wave-operator and the effective Hamiltonian, it is in many-body theory often more efficient to employ iterative or *all-order procedures*, based on the formalism of *second quantization*, a procedure we shall here summarize.

The operators $a_i^\dagger$ and a_i are time-independent single-electron *creation and annihilation operators*, which, respectively, create and annihilate a single-electron part of the many-electron wave function. These operators satisfy the *anti-commutation rules*

$$\begin{aligned} \{a_i^\dagger, a_j^\dagger\} &= a_i^\dagger a_j^\dagger + a_j^\dagger a_i^\dagger = 0 \\ \{a_i, a_j\} &= a_i a_j + a_j a_i = 0 \\ \{a_i^\dagger, a_j\} &= a_i^\dagger a_j + a_j a_i^\dagger = \delta_{ij}, \end{aligned} \tag{16}$$

where δ_{ij} is the Kronecker delta factor. A quantum-mechanical operator can then be expanded as

$$\mathcal{O} = C + a_i^\dagger \langle i|\mathcal{O}_1|j\rangle\, a_j + \frac{1}{2!} a_i^\dagger a_j^\dagger \langle ij|\mathcal{O}_2|kl\rangle\, a_l a_k + \cdots = \mathcal{O}_0 + \mathcal{O}_1 + \mathcal{O}_2 + \cdots , \tag{17}$$

where C is a number, representing the *zero-body* part, the next term is the *one-body* part etc. Unless otherwise explicitly stated, we employ here the *summation convention* with *summation over all values of repeated indices appearing only on one side of an equation*. The 'matrix elements' are given by

$$\begin{aligned} \langle i|\mathcal{O}_1|j\rangle &= \int \mathrm{d}\boldsymbol{x}_1\, \phi_i^\dagger(x_1)\, \mathcal{O}_1\, \phi_j(x_1) \\ \langle ij|\mathcal{O}_2|kl\rangle &= \iint \mathrm{d}\boldsymbol{x}_1\, \mathrm{d}\boldsymbol{x}_2\, \phi_i^\dagger(x_1)\phi_j^\dagger(x_2)\, \mathcal{O}_2\, \phi_k(x_1)\phi_l(x_2) \\ &\text{etc.} \end{aligned} \tag{18}$$

where $\mathrm{d}\boldsymbol{x}$ represents the three-dimensional volume element.

Normally, in field theory, a *vacuum level* $|0\rangle$ is defined, related to the empty space with no particles. Then $a_i^\dagger|0\rangle = |i\rangle$ represents a state with a single electron in the electron state i, corresponding to the single-electron function $\phi_i(\boldsymbol{x})$ etc. In nonrelativistic theory all operators then refer to *particles states* (with positive energy). In relativistic theory, also *hole states* (positron states) with negative energy appear.

In many-body atomic or molecular theory it is usually more convenient to *define a vacuum level* $|0\rangle$ *in relation to a suitable closed-shell system (core)*. Then $a_i^\dagger\,|0\rangle$ represents a system with a single electron i outside the core, provided that the electron state i is not present in

the core. Similarly, $a_i\,|0\rangle$ represents a system with a hole in the core, provided the state i is initially present in the core.

We assume that the vacuum is a many-electron state, represented by a single determinant, and we can then separate the single-particle states into the two categories:

– *core states*, occupied in the vacuum state;

– *particle states*, not occupied in the vacuum state.

We also introduce *'particle-hole'* (p-h) operators according to

$$b_i^\dagger = \begin{cases} a_i^\dagger & (i \text{ particle state}) \\ a_i & (i \text{ core state}), \end{cases}$$
$$b_i = \begin{cases} a_i & (i \text{ particle state}) \\ a_i^\dagger & (i \text{ core state}). \end{cases} \tag{19}$$

Thus, *the $b_i^\dagger$ operator creates an electron in a particle state (above the vacuum level) or annihilates an electron in a core state – 'creates a hole' – below the vacuum level and v.v.*

In principle, the operators might be *time dependent* with *time running from right to left*, so that the leftmost operator corresponds to the latest time. We refer to the ordering right-left as the *time ordering*.

In standard field theory a second-quantized operator is said to be *normal ordered* or in *normal form*, if all creation operators appear to the left of the annihilation operators. In the particle-hole formalism ***we define normal order so that all particle-hole creation operators*** ($b^\dagger$) ***appear to the left of the particle-hole creation operators*** (b). We shall use ***curly brackets*** to denote an operator in normal form, $\{A\}$.

Wick's theorem
The order between second-quantized operators can be changed by using the anti-commutation rules (16), which might lead to *contractions*. If x, y are creation/annihilation operators, then *a **contraction** is defined as the difference between the time-ordered and normal-ordered forms*

$$\overbrace{x\,y} = x\,y - \{x\,y\}. \tag{20}$$

From the anti-commutation rules it then follows that

$$\overbrace{a_i^\dagger\,a_j^\dagger} = \overbrace{a_i\,a_j} = \overbrace{a_i^\dagger\,a_j} = 0 \quad \text{and} \quad \overbrace{a_i\,a_j^\dagger} = \delta_{ij}. \tag{21}$$

Wick's theorem [44] states that *a second-quantized operator can be expressed as the normal form plus all possible normal-ordered contractions* (single, double etc)

$$A = \{A\} + \{\overset{\sqcap}{A}\}. \tag{22}$$

All terms are then in normal form.

In applying Wick's theorem for a product of operators, it is convenient first to normal order each of the components. Then the theorem can be formulated as follows [26]:
If A and B are operators in normal form, then the product is equal to the normal product plus all normal-ordered contractions between A and B,

$$A\,B = \{A\,B\} + \{\overset{\sqcap\!\sqcap}{A\,B}\}. \tag{23}$$

No contractions *within* the operators will occur. This form of the theorem is particularly convenient in constructing the many-body diagrams.

Normal form of the perturbation
The perturbation (5) can be expressed in second quantization as

$$H' = a_i^\dagger \langle i| - u|j\rangle\, a_j + \frac{1}{2} a_i^\dagger a_j^\dagger \langle ij|\frac{1}{r_{12}}|kl\rangle\, a_l a_k, \tag{24}$$

(summation over the indices of the creation/annihilation operators being understood) and normal ordering this operator may lead to contractions within the operator. For the one-body term there will be a contraction only if $i = j$ is a core state, which leads to

$$a_i^\dagger \langle i| - u|j\rangle\, a_j = \sum_i^{\text{core}} \langle i| - u|i\rangle + \{a_i^\dagger a_j\} \langle i| - u|j\rangle. \tag{25}$$

This contains a zero-body and a normal-ordered one-body part.

Similarly, the two-body term yields [26, p.240]

$$\begin{aligned}\frac{1}{2} a_i^\dagger a_j^\dagger \langle ij|r_{12}^{-1}|kl\rangle\, a_l a_k &= \sum_{i,j}^{\text{core}} \left[\langle ij|r_{12}^{-1}|ij\rangle - \langle ij|r_{12}^{-1}|ji\rangle\right] \\ + \sum_k^{\text{core}} \{a_i^\dagger a_j\}\left[\langle ik|r_{12}^{-1}|jk\rangle - \langle ik|r_{12}^{-1}|kj\rangle\right] &+ \frac{1}{2}\{a_i^\dagger a_j^\dagger a_l a_k\}\langle ij|r_{12}^{-1}|kl\rangle,\end{aligned} \tag{26}$$

which contains a zero-body and normal-ordered one- and two-body parts. The normal-ordered one-body part in Eq. (26) represents the *Hartree-Fock potential of the core* (vacuum state), v_{HF}. Combined with

the one-body part of the potential term (25), the complete normal-ordered one-body part of the perturbation can be expressed by means of an '*effective potential*',

$$\{a_i^\dagger a_j\}\langle i|v_{\rm eff}|j\rangle = \{a_i^\dagger a_j\}\langle i|v_{\rm HF} - u|j\rangle. \tag{27}$$

Summarizing, the normal-ordered perturbation can be expressed

$$H' = H_0 + H_1 + H_2, \tag{28}$$

where the terms represent the normal-ordered zero-, one- and two-body parts, respectively,

$$\begin{aligned} H_0 &= \sum_i^{\rm core}\langle i| - u|i\rangle + \sum_{i,j}^{\rm core}\left[\langle ij|r_{12}^{-1}|ij\rangle - \langle ij|r_{12}^{-1}|ji\rangle\right] \\ H_1 &= \{a_i^\dagger a_j\}\langle i|v_{\rm eff}|j\rangle = \{a_i^\dagger a_j\}\langle i|v_{\rm HF} - u|j\rangle \\ H_2 &= \frac{1}{2}\{a_i^\dagger a_j^\dagger a_l a_k\}\langle ij|r_{12}^{-1}|kl\rangle. \end{aligned}$$

If the orbitals are generated in the HF potential of the core, i.e., the vacuum for the normal ordering, the one-body part of the normal-ordered perturbation vanishes.

2.3. Graphical representation of MBPT

Graphically, we adopt the convention that

– ***a particle/core state is represented by a line directed up/down***.

A valence (particle or core) state is denoted by double arrows, as shown in Fig. 1, but a single arrow can represent valence as well as nonvalence states.

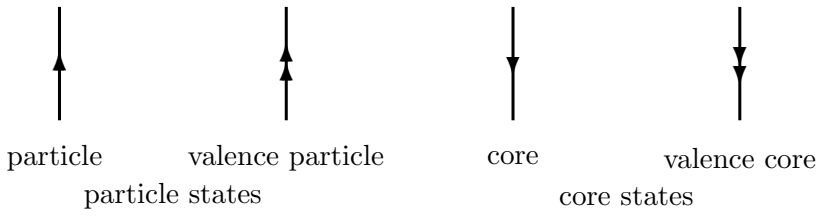

Figure 1. Graphical representation of the four kinds of orbitals.

Furthermore, we assume that

– ***a particle creation/annihilation*** $(a^\dagger/a)$ ***operator is represented by a line directed from/towards a vertex***.

From this it follows that

– ***particle-hole creation/annihilation operators*** $(b^\dagger/b)$ ***appear above/below the vertex.***

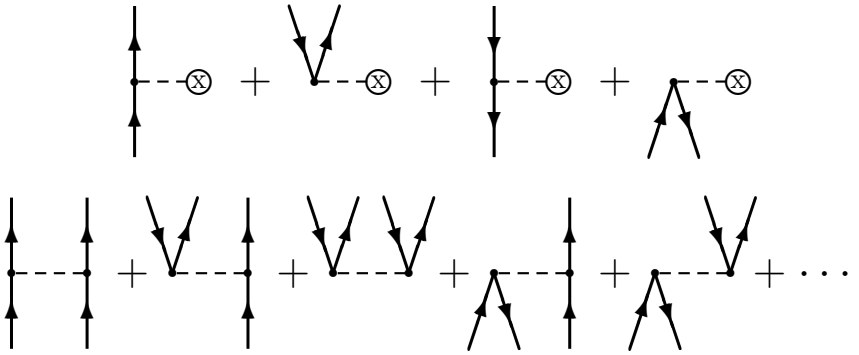

Figure 2. Graphical representation of the normal-ordered one- and two-body parts of the perturbation (28). The dotted line represents the electrostatic interaction between the electrons and the circle with a cross represents the 'effective potential' (27), which vanishes if the orbitals are generated in the HF potential of the core (vacuum state). Lines directed upwards/downwards represent particle/core states.

The only p-h annihilation that can occur when operating on the model space are *valence* p-h annihilation. Thus,

$$b_{\mathrm{non-valence}} P = 0. \tag{29}$$

This implies that *no other free lines than valence lines are allowed at the bottom of a diagram when operating to the right on the model space.* Similarly, no other free lines than valence lines are allowed at the *top* of a diagram when operating to the *left* on the model space. An operator that operates to the right as well as to the left on the model space, PAP, is said to be *closed* and represented by a *closed diagram with no other free lines then valence lines.* A diagram that is not closed is said to be *open.*

A diagram with no free lines at all represents a zero-body operator, a diagram with one line in and out represents a normal-ordered one-body operator etc. The normal-ordered one- and two-body parts of the perturbation (28) are shown in Fig. 2.

2.4. Linked-Diagram expansion

When the perturbation expansion is expressed in second-quantized or diagrammatic form, it is found that so-called *unlinked terms/diagrams* are largely eliminated. *A diagram is said to be unlinked, if it contains a disconnected, closed part.* The cancellation of the unlinked diagrams can be indicated in the following way.

With the operators expressed in normal form, we can apply Wick's theorem in the form (23) on the r.h.s. of the Bloch equation (13), yielding

$$[\Omega, H_0]P = \Big(\{H'\Omega\} + \overbrace{\{H'\Omega\}} - \{\Omega W\} - \overbrace{\{\Omega W\}}\Big)P. \tag{30}$$

The unlinked part of $\{H'\Omega\}$ can be shown to be cancelled by $\{\Omega W\}$, if the model space is *complete*, which implies that it contains all determinants that can be formed by the valence electrons. This leaves

$$[\Omega, H_0]P = \Big(\{H'\Omega\}_{\text{Linked}} + \overbrace{\{H'\Omega\}} - \overbrace{\{\Omega W\}}\Big)P. \tag{31}$$

The first term on the r.h.s. is *disconnected* but still '*linked* with our definitions, since all separate parts are open. The remaining terms would be linked if Ω is linked. Then it can be shown by induction that only linked terms remain, or

$$[\Omega, H_0]P = \big[(H'\Omega - \Omega W)P\big]_{\text{Linked}}. \tag{32}$$

The last term represent co-called *folded diagrams* [6, 26]. Here, the diagrams of Ω and W are connected by one or several valence lines, and the diagrams are conventionally drawn in a "folded" way, as will be illustrated below. Obviously, this terms appears only for open-shell systems with valence particles or holes present.

An even more effective form of MBPT is the *Coupled-Cluster Approach* (CCA), where the wave operator is expressed in exponential form [18, 12, 11, 22], a procedure frequently used in quantum chemistry [10, 36, 2, 39]. For general open-shell systems it is convenient to use the *normal-ordered exponential form* [15, 30, 26]

$$\Omega = \{\mathrm{e}^S\} = 1 + S + \frac{1}{2}\{S^2\} + \cdots \tag{33}$$

(where again the curly brackets are used to denote normal order). All the results we shall derive here are valid also in the coupled-cluster approach, but for simplicity we shall stick to the standard many-body formalism.

Using second quantization, the wave operator can be separated into normal-ordered one-, two-,.. body parts

$$\Omega = 1 + \Omega_1 + \Omega_2 + \dots \tag{34}$$

or

$$\Omega = 1 + \{a_i^\dagger a_j\} x_j^i + \frac{1}{2!} \{a_i^\dagger a_j^\dagger a_l a_k\} x_{kl}^{ij} + \cdots \tag{35}$$

It follows from (10) that *in intermediate normalization all wave-operators terms are open* – except the trivial unit term. The graphical form of the one- and two-body parts is given in Fig. 3, assuming no valence holes. Since the wave operator operates to the right on the model space (29), only valence lines are allowed at the bottom.

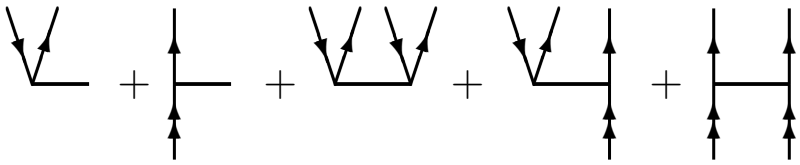

Figure 3. Graphical representation of the one- and two-body parts of the normal-ordered wave operator (35), assuming no valence holes. The diagrams are *open*, which means that all lines are not allowed to be valence lines.

By applying Wick's theorem on the r.h.s. of the Bloch equation (13), the identification, using the partitioning (34), leads to a set of coupled equations

$$[\Omega_n, H_0]P = \left[(H'\Omega - \Omega W)P\right]_{\text{Linked},\, n}. \tag{36}$$

Solving these equations self-consistently, for instance, with the approximation

$$\Omega = 1 + \Omega_1 + \Omega_2, \tag{37}$$

yields the effect of single and double excitations to all orders of perturbation theory. We shall refer to this as the *pair approximation*.

3. MBPT treatment of a single electron outside closed shells

We consider now the special case of a single (valence) electron outside a closed-shell core, and we shall use the MBPT formalism of the previous section to derive the equation for the valence Brueckner orbital. In the next section we shall treat the same problem using the Green's-function or propagator method.

The model space can in this case be restricted to a single determinant (model function) Φ, which is an eigenfunction of H_0 (4),

$$H_0\,\Phi = E_0\,\Phi, \tag{38}$$

and the projection operator for the model space is

$$P = |\Phi\rangle\langle\Phi|. \tag{39}$$

The Bloch equation (32) becomes

$$(E_0 - H_0)\,\Omega P = \big[(H'\Omega - \Omega W)P\big]_{\text{Linked}}, \tag{40}$$

and the coupled equations (36)

$$(E_0 - H_0)\,\Omega_n P = \big[(H'\Omega - \Omega W)P\big]_{\text{Linked},\,n}, \tag{41}$$

where $W = PH'\Omega P$ is the effective interaction (14).

The single target function is given by

$$\Psi = \Omega\Phi \tag{42}$$

and the total energy of the system by

$$E = \langle\Phi|H\Omega|\Phi\rangle = E_0 + \langle\Phi|W|\Phi\rangle. \tag{43}$$

Our vacuum state is chosen to be the ground state of the ion core. We generate the orbitals in the HF potential of the core, which means that the one-body part of the normal-ordered perturbation (28) *vanishes.*

3.1. The pair approximation

With the pair approximation (37) the wave-operator equations (41) become

$$\begin{aligned}
(E_0 - H_0)\,\Omega_1 P &= \big[(H'\Omega - \Omega_1 W_1)P\big]_{\text{Linked},\,1} \\
(E_0 - H_0)\,\Omega_2 P &= \big[(H'\Omega - \Omega_2 W_1)P\big]_{\text{Linked},\,2} \\
W_1 &= (PH'\Omega P)_{\text{Linked},\,1}.
\end{aligned} \tag{44}$$

From the first equation we obtain

$$(\varepsilon_p - \varepsilon_r)\langle\Phi_p^r|\Omega_1|\Phi\rangle = \langle\Phi_p^r|H'\Omega - \Omega_1 W_1|\Phi\rangle_{\text{Linked},\,1}, \tag{45}$$

where Φ_p^r is the a determinant with the occupied orbital p of Φ replaced by an unoccupied (virtual) orbital r. Similarly, the Ω_2 equation is obtained by projecting on the second equation in (44) by a doubly excited function.

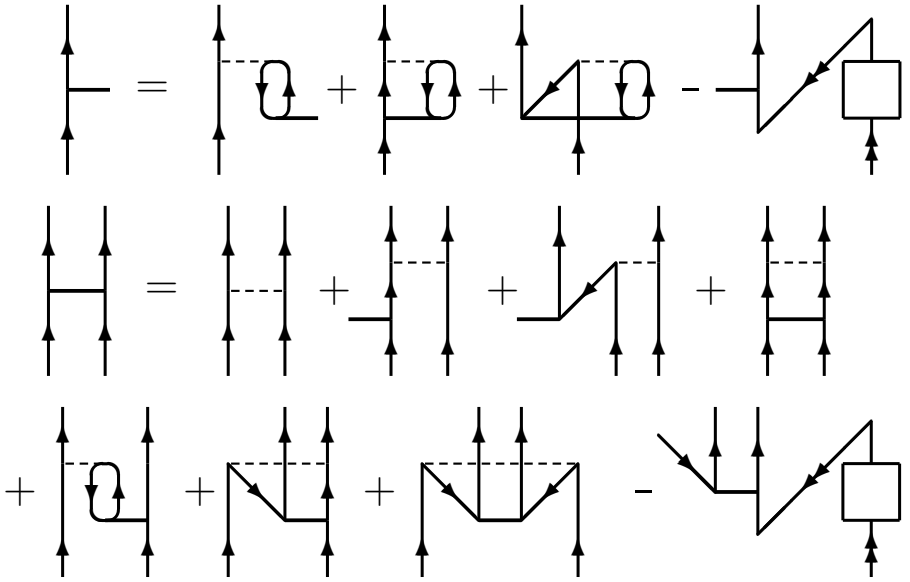

Figure 4. Graphical representation of the Ω_1 and Ω_2 equations in the pair approximation (37) (leaving out exchange variants). The last diagram in each equation is a folded diagram, which appears only when the incoming line is a valence line. The box represents the effective interaction (14). For simplicity, all incoming lines are directed upwards, although at most one incoming orbital can in our case be a valence line.

The graphical form of the equations (44) is given in Fig. 4. Since we have assumed here that the orbitals are generated in the HF potential of the ion core, there is no one-body part of the normal-ordered perturbation (28), and the bare H' term will not contribute to the one-body equation. The first diagram on the r.h.s. of this equation represents $H'\Omega_1$, the next two $H'\Omega_2$ and the last (folded) diagram the term $-\Omega_1 W_1$. The latter appears only when the incoming line is a valence line. Conventionally, the internal valence line of a folded diagram is drawn downwards. In the Ω_2 equation the first diagram represents H', the next two $H'\Omega_1$, the next four $H'\Omega_2$ and the last diagram the folded term $-\Omega_2 W_1$. Since there is only one valence electron in our case, the effective interaction in the folded diagram can only be of one-body type. Exchange variants are left out.

3.2. The removal energy

The total energy of our system is according to Eq. (43) given by the zeroth-order energy in addition to the expectation value of the effective

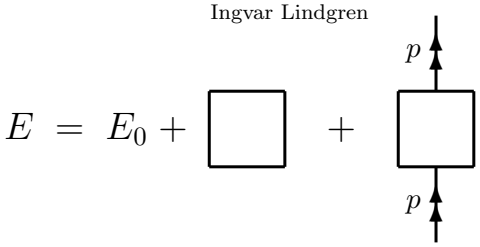

Figure 5. Total energy of a system with a single electron outside a core of closed shells is given by the zeroth-order energy and the zero-body and the one-body parts of the effective interaction W (14). The latter parts are given in more detail in Fig. 6.

interaction W in the model state. Since $W = PH'\Omega P$, we obtain the corresponding graphical representation by *'closing'* the diagrams of the wave operator Ω by operating with the perturbation H', so that no other free lines than valence lines should appear. Since in the present case we have only one valence line, this can result in *zero-order diagrams* with no free lines, representing the zero-body part of the effective interaction W, W_0, and *one-body diagrams* with a single valence line in and out, representing the one-body part, W_1, as illustrated in Fig: 5. The one- and two-body parts are illustrated in more details in Fig. 6.

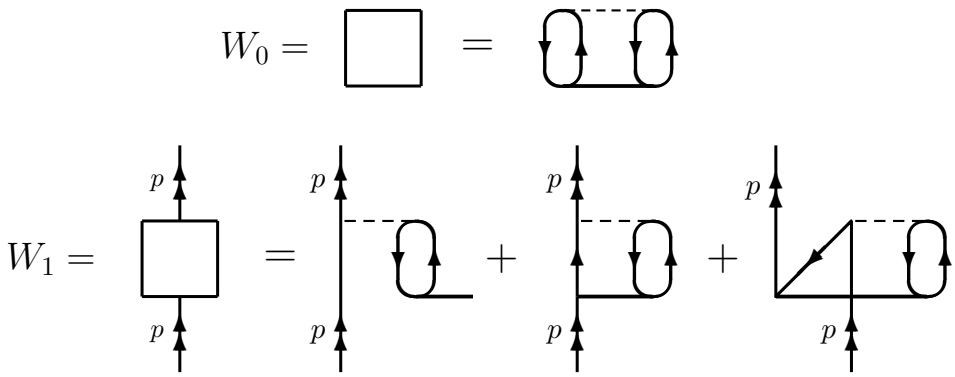

Figure 6. Graphical representation of the zero-body (W_0) and one-body (W_1) parts of the effective interaction (14), obtained by 'closing' the diagrams of the wave operator by the perturbation H'. The zero-body part has no free lines at all and the one-body part a single valence line (p) in and out, but no other free lines (self-energy diagrams). Exchange variants are left out.

Since there is no one-body part of the normal-ordered perturbation in our case, the zero-body part of the effective interaction can only be achieved by closing the *two-body* part of the wave operator (33), as is

illustrated in the top line of Fig. 6. The bottom line of the figure shows the one-body part of the effective interaction.

Figure 7. Total energy of the ion core is given by the zeroth-order energy and the zero-body part W_0 of the effective interaction (14), i.e., closed diagrams with no free lines. The zero-body part is in our formalism identical to that of the neutral system in Fig. 5.

The total energy of the ion core, which is a closed-shell system, is given by the zeroth-order energy of that system and the *zero-body* part (W_0) of the effective interaction, as illustrated in Fig. 7. We employ here the ***principle of valence universality*** [27], which implies that *the wave-operator amplitudes are independent of the degree of ionization*. Therefore, the zero-body parts of the effective interaction are identical for the neutral and ionized systems.

The *removal energy* of the valence electron is given by the difference between the total energies of the neutral system and the ion core

$$-BE = E - E^{\rm core}. \tag{46}$$

Since the zero-body contributions cancel, it follows that ***the removal energy is given by the orbital (HF) eigenvalue and the one-body part of the effective interaction***,

$$-BE = \varepsilon_p + \langle\Phi|W_1|\Phi\rangle, \tag{47}$$

as illustrated in Fig. 8. This is the ***exact ionization energy, including correlation as well as relaxation effects***. The one-body diagrams are shown more explicitly in Fig. 6, where the second diagram represents the correlation effect and the last diagram the relaxation, i.e., the effect due to modification of the core orbitals at the removal of the valence electron.

The one-body part of the effective interaction is of self-energy (SE) type and can be expressed as the expectation value of a *self-energy operator*

$$\langle\Phi|W_1|\Phi\rangle = \langle\Phi|H'\Omega|\Phi\rangle_{\rm Linked,1} = \langle p|\Sigma(\varepsilon_p)|p\rangle. \tag{48}$$

Defining

$$\delta\varepsilon_p = \langle\Phi|W_1|\Phi\rangle = \langle p|\Sigma(\varepsilon_p)|p\rangle, \tag{49}$$

the (negative of the) removal energy is from (47)

$$-BE = \varepsilon_p + \delta\varepsilon_p. \tag{50}$$

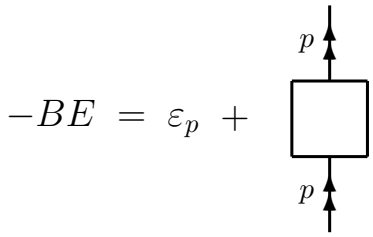

Figure 8. The (negative of the) removal energy of the valence electron is given by the orbital Hartree-Fock eigenvalue in addition to the one-body part (W_1) of the effective interaction (14). The diagrammatic representation of the latter is given in Fig. 6. This includes proper as well as improper self-energy diagrams.

3.3. Brueckner and Dyson orbitals

Single excitations represented by the single-particle equation (45) and the top line in Fig. 4 are one-body effects and can therefore in principle be included in a single-particle model. We shall now consider such excitations from the valence state (p) in some detail.

We start with the single-particle equation (45)

$$(\varepsilon_p - \varepsilon_r)\langle\Phi_p^r|\Omega_1|\Phi\rangle = \big[\langle\Phi_p^r|H'\Omega|\Phi\rangle - \langle\Phi_p^r|\Omega_1|\Phi\rangle\langle\Phi|W_1|\Phi\rangle\big]_{\text{Linked},1}, \quad (51)$$

where we have inserted the projection operator for the model space (39), $P = |\Phi\rangle\langle\Phi|$, in the last term. The matrix element $\langle\Phi_p^r|\Omega_1|\Phi\rangle$ is the amplitude of the Ω_1 operator for the single excitation $p \to r$ and is graphically represented by the Ω_1 diagrams in Fig. 4. Using the definition (49), we can express the folded term above as $-\delta\varepsilon_p\,\langle\Phi_p^r|\Omega_1|\Phi\rangle$, and Eq. (51) then becomes

$$(\varepsilon_p + \delta\varepsilon_p - \varepsilon_r)\langle\Phi_p^r|\Omega_1|\Phi\rangle = \langle\Phi_p^r|H'\Omega|\Phi\rangle_{\text{Linked},1}. \quad (52)$$

Thus, we see that the effect of the folded term is simply to shift the energy denominator of the Ω_1 operator by the amount $\delta\varepsilon_p$. We can then leave out the folded part of the Ω_1 equation, if we make the following replacement in the energy denominator,

$$\varepsilon_p \to \varepsilon_p^* = \varepsilon_p + \delta\varepsilon_p. \quad (53)$$

Using the self-energy operator, the result can be expressed in analogy with the one-body effective interaction (48) as

$$(\varepsilon_p^* - \varepsilon_r)\langle\Phi_p^r|\Omega_1|\Phi\rangle = \langle r|\Sigma(\varepsilon_p)|p\rangle, \quad (54)$$

defining the general SE operator by

$$\langle r|\Sigma(\varepsilon_p)|p\rangle = \langle\Phi_p^r|H'\Omega|\Phi\rangle_{\text{Linked},1} \quad (55)$$

(which is consistent with the definition of the diagonal part (49)). This is illustrated in Fig. 9. This can also represent the Ω_1 amplitude, if we apply the *modified* denominator (53).

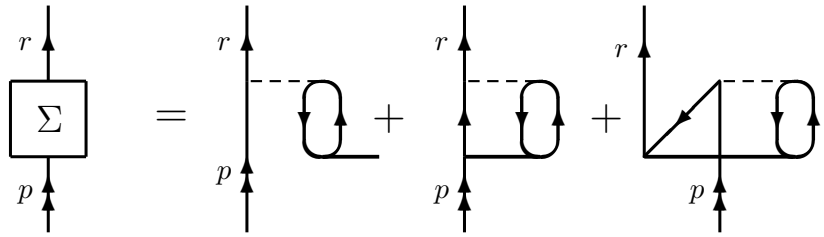

Figure 9. Graphical representation of the nondiagonal part of the self-energy operator $\Sigma(\varepsilon_p)$. This representation is analogous to the diagonal part shown in Fig. 6 (no folded part). This can also represent the corresponding part of the wave operator, if we apply the *modified* energy shift (53). As before, exchange variants are left out.

We can now form a new orbital for the valence electron by adding the contribution (54) to the HF orbital,

$$\phi_p^*(\boldsymbol{x}) = \langle \boldsymbol{x}|p^*\rangle = \langle \boldsymbol{x}|p\rangle + \langle \boldsymbol{x}|r\rangle\langle\Phi_p^r|\Omega_1|\Phi\rangle = \langle \boldsymbol{x}|p\rangle + \frac{\langle \boldsymbol{x}|r\rangle\langle r|\Sigma(\varepsilon_p)|p\rangle}{\varepsilon_p^* - \varepsilon_r}. \tag{56}$$

By replacing the HF orbital of the valence electron in the determinant Φ by the modified orbital, $\phi_p^*(\boldsymbol{x})$, ***all single excitations from the valence electron of the exact wave function will be included***. Therefore, ***the modified orbital is the Brueckner orbital for the valence electron*** [7, 32, 28].

In order to show more explicitly that the modified orbital (56) is a Brueckner orbital, we can form a single excitation from the modified valence orbital p^* into a virtual orbital s^*, which we denote by $\Phi_p^{s^*}$. The virtual orbital must be orthogonalized against the modified valence orbital, i.e.,

$$\langle s^*|p^*\rangle = \langle s^*|p\rangle + \langle s^*|r\rangle\langle\Phi_p^r|\Omega_1|\Phi\rangle = 0. \tag{57}$$

But this can also be expressed

$$\big\langle \Phi_p^{s^*}\big|\big[|\Phi\rangle + |\Phi_p^r\rangle\langle\Phi_p^r|\Omega_1|\Phi\rangle\big] = \big\langle \Phi_p^{s^*}\big|\Psi\big\rangle = 0, \tag{58}$$

which is the ***Brillouin-Brueckner or maximum-overlap condition for the valence electron*** [7, 32].

We consider here only the Brueckner orbital for the valence electron, while the core orbitals are left as HF orbitals. The modified valence orbital then satisfies the maximum-overlap condition with the core orbitals frozen.

When the SE diagrams are generated perturbatively by inserting the iterated one- and two-body wave-operator parts in the expansion in Fig. 9, also *improper* SE parts can appear, i.e., parts that can be separated into two allowed SE parts by cutting a single orbital line. When such a separation is not possible, the SE part is said to be *proper*. Therefore, the general SE operator can be expanded in terms of proper SE parts, as illustrated in Fig. 10. We assume here that the energy denominators of the single-particle equation are evaluated by means of the modified energy (53), which eliminates folded diagrams from the expansion, so that the intermediate lines (s) in the figure are virtual (non-valence) lines.

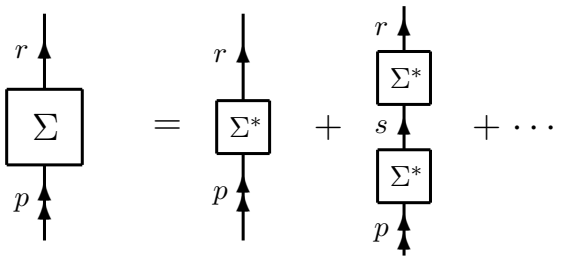

Figure 10. The general self energy (Σ) can be expanded in proper self energies (Σ^*). The energy denominators are evaluated by means of the modified energy (53), which implies that there are no folded diagrams in the expansion.

Using the *proper* self energy, the Brueckner-orbital equation (56) can be expressed in the form of a *Dyson equation*

$$\langle \boldsymbol{x}|p^*\rangle = \langle \boldsymbol{x}|p\rangle + \frac{\langle \boldsymbol{x}|r\rangle\langle r|\Sigma^*(\varepsilon_p)|p^*\rangle}{\varepsilon_p^* - \varepsilon_r}, \tag{59}$$

where the Brueckner orbital appears also on the r.h.s. of the equation. This is illustrated in Fig. 11. We recall that r represents here *virtual* state, i.e., a particle state different from the valence state (p).

The Brueckner orbital (59) satisfies the differential equation

$$(\varepsilon_p^* - h_0)\langle \boldsymbol{x}|p^*\rangle = (\varepsilon_p^* - h_0)\langle \boldsymbol{x}|p\rangle + \langle \boldsymbol{x}|r\rangle\langle r|\Sigma^*(\varepsilon_p)|p^*\rangle. \tag{60}$$

Using the definition (53), the first term on the r.h.s. can be expressed

$$(\varepsilon_p^* - h_0)\langle \boldsymbol{x}|p\rangle = \delta\varepsilon_p\langle \boldsymbol{x}|p\rangle,$$

since $h_0\langle \boldsymbol{x}|p\rangle = \varepsilon_p\langle \boldsymbol{x}|p\rangle$. According to the relation (49), $\delta\varepsilon_p$ is equal to the diagonal element of the SE operator, which we can also express in terms of the proper SE and the Brueckner orbital

$$\delta\varepsilon_p = \langle p|\Sigma(\varepsilon_p)|p\rangle = \langle p|\Sigma^*(\varepsilon_p)|p^*\rangle. \tag{61}$$

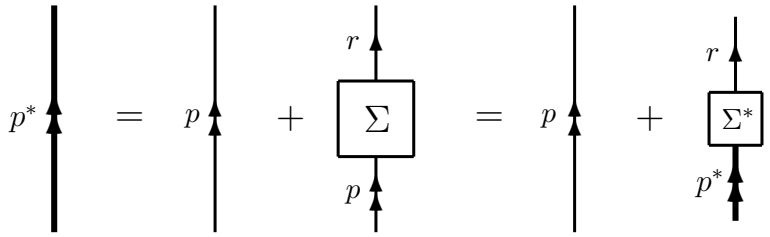

Figure 11. Dyson equation for generating the Brueckner valence orbital (56). The thick line represents the Brueckner orbital and the thinner lines HF orbitals. The large box represents the general self energy (Σ) and the small box the proper self energy (Σ^*).

This leads to

$$(\varepsilon_p^* - h_0)\langle \boldsymbol{x}|p^*\rangle = \langle \boldsymbol{x}|r\rangle\langle r|\Sigma^*(\varepsilon_p)|p^*\rangle, \tag{62}$$

summed over all particle states, *including* the valence orbital but excluding core states. But it follows from the definition (55) that the matrix element

$$\langle i|\Sigma(\varepsilon_p)|p\rangle = \langle \Phi_p^i|H'\Omega|\Phi\rangle_{\text{Linked,1}} = \langle i|\Sigma^*(\varepsilon_p)|p^*\rangle = 0,$$

when i is a core state, since $\langle\Phi_p^i|$ would then vanish. Therefore, we can let the sum in (62) run over *all* states, and using the identity $\sum_{\text{all i}} |i\rangle\langle i| = 1$, this yields

$$(\varepsilon_p^* - h_0)\langle \boldsymbol{x}|p^*\rangle = \langle \boldsymbol{x}|\Sigma^*(\varepsilon_p)|p^*\rangle. \tag{63}$$

The self-energy operator is obtained by forming a one-body operator by operating with the perturbation on the wave operator. In principle, this will contain also folded diagrams. We have seen that the folded diagram of the single-particle equation in Fig. 4 has the effect of modifying the energy denominator of the Ω_1 operator, when the valence electron is being excited. This is true also for the S_2 equation, and we can leave out the folded diagram also from this equation, if we make the same energy-denominator shift (53). This has the effect that the energy parameter of the SE operator will be shifted in the same way,

$$\Sigma^*(\varepsilon_p) \to \Sigma^*(\varepsilon_p^*), \tag{64}$$

and then no folded diagrams from the S_2 equation will appear. Then the expressions (56) and (59) for the Brueckner orbital become

$$\langle \boldsymbol{x}|p^*\rangle = \langle \boldsymbol{x}|p\rangle + \frac{\langle \boldsymbol{x}|i\rangle\langle i|\Sigma(\varepsilon_p^*)|p\rangle}{\varepsilon_p^* - \varepsilon_i} = \langle \boldsymbol{x}|p\rangle + \frac{\langle \boldsymbol{x}|i\rangle\langle i|\Sigma^*(\varepsilon_p^*)|p^*\rangle}{\varepsilon_p^* - \varepsilon_i}, \tag{65}$$

where according to the discussion above, i can run over *all* orbitals. Similarly, the Dyson equation (63) becomes

$$(\varepsilon_p^* - h_0)\langle \boldsymbol{x}|p^*\rangle = \langle \boldsymbol{x}|\Sigma^*(\varepsilon_p^*)|p^\rangle. \tag{66}$$

This can also be expressed

$$h_0\,\langle \boldsymbol{x}|p^*\rangle + \langle \boldsymbol{x}|\Sigma^*(\varepsilon_p^*)|\boldsymbol{x'}\rangle\langle \boldsymbol{x'}|p^*\rangle = \varepsilon_p^*\langle \boldsymbol{x}|p^*\rangle \tag{67}$$

or in integral form

$$h_0\,\phi_p^*(\boldsymbol{x}) + \int \mathrm{d}\boldsymbol{x'}\,\Sigma^*(\boldsymbol{x},\boldsymbol{x'},\varepsilon_p^*)\,\phi_p^*(\boldsymbol{x'}) = \varepsilon_p^*\,\phi_p^*(\boldsymbol{x}). \tag{68}$$

Here, $\langle \boldsymbol{x}|\Sigma^*(\varepsilon_p^*)|\boldsymbol{x'}\rangle = \langle \boldsymbol{x}|\Sigma^*(\varepsilon_p^*)|\boldsymbol{x'}\rangle$ is the proper self energy in the coordinate representation. Eq. (67)/(68) is the eigenvalue equation of the Brueckner orbital for the valence electron, and according to the relation (50) ***the eigenvalue ε_p^* represents the exact removal energy of the valence electron***. $\Sigma^*(\boldsymbol{x},\boldsymbol{x'},\varepsilon_p^*)$ is the nonlocal potential of the Brueckner orbital, discussed in by Lindgren and Salomonson [28].

The solution of the Dyson equation (67) is known also as the *Dyson orbital* [35], and it follows from the present analysis that ***for a single valence electron outside closed shells the Brueckner and Dyson orbitals are identical concepts***.

The treatment above holds also for a state with a single *hole* in a closed-shell core, and the eigenvalue then represents the corresponding *electron affinity*. It will also hold in principle under more general conditions, as will be demonstrated in a forthcoming publication.

3.4. Application to the alkali atoms

As an illustration of the procedure descried above, we consider some calculations on the alkali atoms. For lithium ground state and first excited state, our calculation [31] yields about 99% of the many-body effect, i.e., relaxation and correlation effects. The remaining effect is manly due to three-body effects. A similar calculation by Johnson et al. [19] was performed only to third order, which yielded 95-97 % of the effect. Later Blundell et al. [5] have performed a relativistic all-order calculations with singles and doubles (no coupled clusters), which yielded essentially the same result as that of Lindgren. Kaldor et al. [14] have more recently performed relativistic coupled-cluster calculations on all the alkali atoms, yielding about 99 % of the many-body effect for $2s$ but only 96 % for the $2p$ state.

For the ground state of the sodium atom, a very accurate calculation has been performed by Salomonson and Ynnerman [41]. This

Table I. Binding energies for the Li and Na atoms (micro Hartrees)

	Lithium			**Sodium**	
	2^2S	2^2P	Ref.	3^2S	Ref.
Expt'l	198 159	130 246		188 163	
Hartree-Fock	196 304	128 637		182 873	
Difference	1 854	1 609		6 830	
Many-Body calc.	1 850	1 584	[31]	6 840	[41]
	1 855	1 582	[5]	6 399	[19]
	1 835	1 534	[14]	6 385	[14]

is a singles-and-doubles-coupled-cluster calculation (CCSD), but also important three-body clusters are included. The three-body effects were found to be particularly important in this case and amounted to as much as 6 % of the many-body effect. With these effects included, 99.85 % of the many-body effect could be accounted for. The calculations of Johnson et al. and of Kaldor et al. do not include any three-body effects.

4. The propagator or Green's-function method

4.1. Definition of the Green's function

In this section we shall consider the same problem as in the previous section, using the propagator or Green's-function method [24]. As before, we consider a single electron outside closed shells, and we define the ion core as the vacuum state for the second quantization.

Using the creation/annihilation operators (16) and the orbitals (6), we define the *electron field operators* in the Schrödinger representation by

$$\hat{\psi}_{\rm S}(\boldsymbol{x}) = a_j\,\phi_j(\boldsymbol{x}); \quad \hat{\psi}^\dagger_{\rm S}(\boldsymbol{x}) = a^\dagger_j\,\phi^*_j(\boldsymbol{x}), \tag{69}$$

using the summation convention mentioned before. In the *Heisenberg picture* (HP), the wavefunctions are time independent and the time-dependence is transferred to the operators,

$$\Psi_{\rm H} = \Psi_{\rm S}(t=0) = {\rm e}^{{\rm i}Ht}\Psi_{\rm S}(x); \qquad O_H = {\rm e}^{{\rm i}Ht}O_{\rm S}\,{\rm e}^{-{\rm i}Ht}. \tag{70}$$

With the partitioning (3) the operators and wavefunctions in the *interaction picture* (IP) are related to those in the Schrödinger picture

by

$$\Psi_{\rm I}(t) = {\rm e}^{{\rm i}H_0 t}\,\Psi_{\rm S}(t); \qquad O_{\rm I}(t) = {\rm e}^{{\rm i}H_0 t}\,O_{\rm S}\,{\rm e}^{-{\rm i}H_0 t}. \tag{71}$$

In this picture the electron-field operators (69) become

$$\begin{aligned}\hat{\psi}_{\rm I}(x) &= {\rm e}^{{\rm i}H_0 t}\,a_j\,\phi_j(\boldsymbol{x})\,{\rm e}^{-{\rm i}H_0 t} = a_j\,\phi_j(\boldsymbol{x})\,{\rm e}^{-{\rm i}\varepsilon_j t} = a_j\,\langle\boldsymbol{x}|j\rangle\,{\rm e}^{-{\rm i}\varepsilon_j t}\\ \hat{\psi}^\dagger_{\rm I}(x) &= a^\dagger_j\,\phi^*_j(\boldsymbol{x})\,{\rm e}^{{\rm i}\varepsilon_j t} = a^\dagger_j\,\langle j|\boldsymbol{x}\rangle\,{\rm e}^{{\rm i}\varepsilon_j t}.\end{aligned} \tag{72}$$

The *single-particle Green's function* is defined [16, p.64]

$${\rm i}G(x,x_0) = \frac{\langle 0|T[\hat{\psi}_{\rm H}(x)\hat{\psi}^\dagger_{\rm H}(x_0)]|0\rangle}{\langle 0|\,0\rangle}, \tag{73}$$

where $\hat{\psi}_{\rm H}(x)$ is the electron field operator and $|0\rangle$ the vacuum state (in our case the exact ground state of the ion core) in the Heisenberg picture, and T is the time-ordering operator, which orders the operators with increasing time from right to left (obeying the anti-commutation rules (16)). Assuming the vacuum state to be normalized, this can be expressed

$${\rm i}G_0(x,x_0) = \langle 0|\Theta(t{-}t_0)\,\hat{\psi}_{\rm H}(x)\hat{\psi}^\dagger_{\rm H}(x_0){-}\Theta(t_0{-}t)\,\hat{\psi}^\dagger_{\rm H}(x_0)\hat{\psi}_{\rm H}(x)|0\rangle, \tag{74}$$

where $\Theta(t-t_0)$ is the step function (=1 if $t > t_0$ and =0 if $t < t_0$).

4.2. The Fourier transform of the Green's function

We consider first the *retarded Green's function* for which $t > t_0$,

$${\rm i}G_+(x,x_0) = \langle 0|\hat{\psi}_{\rm H}(x)\hat{\psi}^\dagger_{\rm H}(x_0)|0\rangle. \tag{75}$$

Inserting a complete set of eigenstates of the full Hamiltonian with a single electron outside the vacuum (core),

$$H|\Psi_n\rangle = E_n|\Psi_n\rangle \tag{76}$$

and transforming back to the Schrödinger representation (70), leads to the *Lehmann representation*

$$\begin{aligned}{\rm i}G_+(x,x_0) &= \langle 0|{\rm e}^{{\rm i}Ht}\hat{\psi}_{\rm S}(x)\,{\rm e}^{-{\rm i}Ht}|\Psi_n\rangle\langle\Psi_n|{\rm e}^{{\rm i}Ht_0}\hat{\psi}^\dagger_{\rm S}(x_0)\,{\rm e}^{-{\rm i}Ht_0}|0\rangle\\ &= \langle 0|\hat{\psi}_{\rm S}(x)|\Psi_n\rangle\,{\rm e}^{-{\rm i}\tau\Delta E_n}\langle\Psi_n|\hat{\psi}^\dagger_{\rm S}(x_0)|0\rangle\end{aligned} \tag{77}$$

with $\tau = t - t_0$ and $\Delta E_n = E_n - E_{\rm core}$ being the full energy change due to the additional particle ($E_{\rm core}$ is the energy of the core or vacuum state).

With a small *adiabatic damping*, $\mathrm{e}^{-\gamma\tau}$, we can perform the *Fourier transform* of the Lehmann function (77), yielding

$$G_+(\boldsymbol{x},\boldsymbol{x}_0,E)=\int_0^\infty \mathrm{d}\tau\,\mathrm{e}^{\mathrm{i}E\tau}\,G_+(\boldsymbol{x},\boldsymbol{x}_0,\tau)=\frac{\langle 0|\hat{\psi}_{\mathrm{S}}(\boldsymbol{x})|\Psi_n\rangle\,\langle\Psi_n|\hat{\psi}^\dagger_{\mathrm{S}}(\boldsymbol{x}_0)|0\rangle}{E-\Delta E_n+\mathrm{i}\gamma}, \tag{78}$$

where we have used the relation

$$\int_0^\infty \mathrm{d}t\,\mathrm{e}^{\mathrm{i}\alpha t}\,\mathrm{e}^{-\gamma t}=\frac{\mathrm{i}}{\alpha+\mathrm{i}\gamma}. \tag{79}$$

This shows that ***the poles of the retarded single-particle Green's function represent the full energy spectrum of the additional particle***, including all kinds of many-body effects.

Similarly, we can consider the *advanced Green's function* for which $t<t_0$,

$$\mathrm{i}G_-(x,x_0)=-\langle 0|\hat{\psi}^\dagger_{\mathrm{H}}(x_0)\hat{\psi}_{\mathrm{H}}(x)|0\rangle. \tag{80}$$

Inserting a complete set of intermediate states with a single *hole* in the vacuum,

$$H|\Psi_h\rangle=E_h|\Psi_h\rangle, \tag{81}$$

leads to the Fourier transform

$$G_-(\boldsymbol{x},\boldsymbol{x}_0,E)=\int_\infty^0 \mathrm{d}\tau\,\mathrm{e}^{\mathrm{i}E\tau}\,G_-(\boldsymbol{x},\boldsymbol{x}_0,\tau)=-\frac{\langle 0|\hat{\psi}^\dagger_{\mathrm{S}}(\boldsymbol{x})|\Psi_h\rangle\,\langle\Psi_h|\hat{\psi}_{\mathrm{S}}(\boldsymbol{x}_0)|0\rangle}{E-\Delta E_h-\mathrm{i}\gamma}. \tag{82}$$

This shows that the poles of the *advanced* single-particle Green's function represent the energy spectrum of a single *hole* in the core.

4.3. The perturbation expansion

In the interaction picture, using intermediate normalization, the Green's function (73) can be expanded in the following way [16, Eq. 9.5]

$$\mathrm{i}G(x,x_0)=\sum_{n=0}^\infty\frac{(-\mathrm{i})^n}{n!}\int_{-\infty}^\infty \mathrm{d}^4x_1\cdots\int_{-\infty}^\infty \mathrm{d}^4x_n\,\Big\langle\Phi_0\Big|\,T\Big[\mathcal{H}'(x_1)\cdots \cdots\mathcal{H}'(x_n)\,\hat{\psi}_{\mathrm{I}}(x)\hat{\psi}^\dagger_{\mathrm{I}}(x_0)\Big]\Big|\Phi_0\Big\rangle_{\mathrm{conn}}, \tag{83}$$

where Φ_0 is the unperturbed ground state of the vacuum or the ion core (single determinant) and $\hat{\psi}_{\mathrm{I}}(x)$ is the electron field operator in the interaction picture. With $H'_{\mathrm{I}}(t)$ being the perturbation (5), $\mathcal{H}'(x)$ is defined as the *perturbation density* in this picture by

$$H'_{\mathrm{I}}(t)=\int \mathrm{d}\boldsymbol{x}\,\mathcal{H}'(x). \tag{84}$$

The expansion (83) is an alternative formulation of the *linked-diagram theorem* (40), discussed in section 2. The unlinked diagrams are here exactly cancelled by the denominator in (73). (In this case there is no distinction between the concepts of '*connected*' and '*linked*' diagrams).

The *zeroth-order Green's function* or *electron propagator* is given by

$$\mathrm{i}G_0(\boldsymbol{x},\boldsymbol{x}_0,\tau) = \langle\Phi_0|\hat{T}[\hat{\psi}_{\mathrm{I}}(x)\hat{\psi}^\dagger_{\mathrm{I}}(x_0)]|\Phi_0\rangle = \overbrace{\hat{\psi}_{\mathrm{I}}(x)\hat{\psi}^\dagger_{\mathrm{I}}}(x_0) \qquad (85)$$

with $\tau = t - t_0$, which represents a *contraction* (20) between the annihilation and creation field operators. Using the form (72) of the field operators, this can also be expressed in analogy with (74) as

$$\mathrm{i}G_0(\boldsymbol{x},\boldsymbol{x}_0,\tau) = \Theta(\tau)\,\langle\boldsymbol{x}|p'\rangle\langle p'|\boldsymbol{x}_0\rangle\,\mathrm{e}^{-\mathrm{i}\varepsilon_{p'}\tau} - \Theta(-\tau)\,\langle\boldsymbol{x}|h'\rangle\langle h'|\boldsymbol{x}_0\rangle\mathrm{e}^{-\mathrm{i}\varepsilon'_h\tau}, \quad (86)$$

summed over single-electron particle (p') and hole (h') states with positive and negative energy, respectively. The Fourier transform is obtained in analogy with (78) and (82)

$$G_0(\boldsymbol{x},\boldsymbol{x}_0,E) = \frac{\langle\boldsymbol{x}|i\rangle\langle i|\boldsymbol{x}_0\rangle}{E-\varepsilon_i+\mathrm{i}\gamma_i}, \qquad (87)$$

summed over the entire unperturbed single-particle spectrum (6). Here, γ_i is a small quantity, which is positive/negative when i is a particle/hole state. In analogy with the self-energy operator above, this can be regarded as the *coordinate representation* of a *Green's-function operator*, $\hat{G}_0(E)$,

$$G_0(\boldsymbol{x},\boldsymbol{x}_0,E) = \langle\boldsymbol{x}|\hat{G}_0(E)|\boldsymbol{x}_0\rangle \qquad (88)$$

with

$$\hat{G}_0(E) = \frac{|i\rangle\langle i|}{E-\varepsilon_i+\mathrm{i}\gamma_i}. \qquad (89)$$

Using the closure property

$$\langle\boldsymbol{x}|i\rangle\langle i|\boldsymbol{x}_0\rangle = \sum_i^{\mathrm{all}} \phi_i^*(\boldsymbol{x})\,\phi_i(\boldsymbol{x}_0) = \delta(\boldsymbol{x}-\boldsymbol{x}_0),$$

we have from the relation (87)

$$(E-h_0)\,G_0(\boldsymbol{x},\boldsymbol{x}_0,E) = \delta(\boldsymbol{x}-\boldsymbol{x}_0), \qquad (90)$$

an equation often used as the definition of the unperturbed or zeroth-order Green's function.

4.4. The Dyson equation

Applying Wick's theorem to the expansion (83), leads to terms that can be represented by diagrams in very much the same way as in the MBPT expansion in the previous section (see, for instance, [16, Sect.9]). The main difference from MBPT is that the diagrams are *Feynman diagrams*, including all possible time orderings between the interactions, rather than time-ordered Goldstone diagrams. Furthermore, the in- and outgoing free lines represent unperturbed single-electron propagators or single-particle Green's functions rather than single-electron orbitals.

The exact (retarded) single-particle Green's function is represented by all connected diagrams with one incoming and one outgoing free line (representing the zeroth-order Green's function), as illustrated in Fig. 12. This is quite analogous to the Dyson equation illustrated in Fig. 11

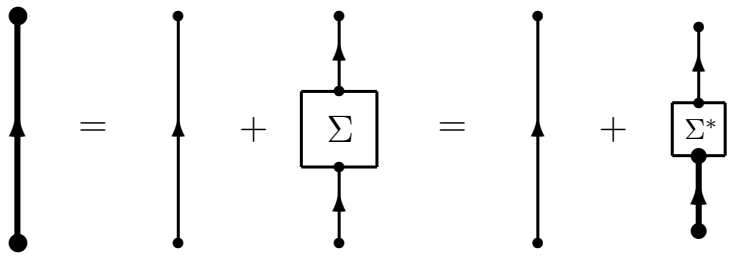

Figure 12. Graphical representation of the Dyson equation for the (retarded) single-particle Green's function. The thick line with dots at the end represents the exact Green's function and the thin lines the zeroth-order Green's function. This relation is quite analogous to the Dyson equation for the Brueckner orbital, represented in Fig. 11.

and corresponds to the Dyson equation

$$\begin{aligned} G(x,x_0) &= G_0(x,x_0) + \iint \mathrm{d}^4x_2\,\mathrm{d}^4x_1\, G_0(x,x_2)\,\Sigma(x_2,x_1)\,G_0(x_1,x_0) \\ &= G_0(x,x_0) + \iint \mathrm{d}^4x_2\,\mathrm{d}^4x_1\, G_0(x,x_2)\,\Sigma^*(x_2,x_1)\,G(x_1,x_0), \end{aligned} \tag{91}$$

where $\Sigma(x_2,x_1)$ is the general and $\Sigma^*(x_2,x_1)$ the proper self energy. After the Fourier transforms this becomes, using the form (88) of the coordinate representations,

$$\begin{aligned} \langle \boldsymbol{x}|\hat{G}(E)|\boldsymbol{x}_0\rangle &= \langle \boldsymbol{x}|\hat{G}_0(E)|\boldsymbol{x}_0\rangle + \langle \boldsymbol{x}|\hat{G}_0(E)|\boldsymbol{x}_2\rangle\,\langle \boldsymbol{x}_2|\Sigma(E)|\boldsymbol{x}_1\rangle\,\langle \boldsymbol{x}_1|\hat{G}_0(E)|\boldsymbol{x}_0\rangle \\ &= \langle \boldsymbol{x}|\hat{G}_0(E)|\boldsymbol{x}_0\rangle + \langle \boldsymbol{x}|\hat{G}_0(E)|\boldsymbol{x}_2\rangle\,\langle \boldsymbol{x}_2|\Sigma^*(E)|\boldsymbol{x}_1\rangle\,\langle \boldsymbol{x}_1|\hat{G}(E)|\boldsymbol{x}_0\rangle, \end{aligned} \tag{92}$$

where as before $|\boldsymbol{x}\rangle\langle\boldsymbol{x}|$ represents space integration over $\boldsymbol{x}$.

Letting the first equation above operate to the right on the valence state $\langle \boldsymbol{x}_0|p\rangle$, using the relation (87), yields

$$\langle \boldsymbol{x}|\hat{G}(E)|\boldsymbol{x}_0\rangle\,\langle \boldsymbol{x}_0|p\rangle = \frac{\langle \boldsymbol{x}|p\rangle}{E-\varepsilon_p+\mathrm{i}\gamma} + \langle \boldsymbol{x}|\hat{G}_0(E)|\boldsymbol{x}_2\rangle\langle \boldsymbol{x}_2|\Sigma(E)\,|\boldsymbol{x}_1\rangle\frac{\langle \boldsymbol{x}_1|p\rangle}{E-\varepsilon_p+\mathrm{i}\gamma}$$

or

$$(E-\varepsilon_p)\langle \boldsymbol{x}|\hat{G}(E)|\boldsymbol{x}_0\rangle\langle \boldsymbol{x}_0|p\rangle = \langle \boldsymbol{x}|p\rangle + \langle \boldsymbol{x}|\hat{G}_0(E)|\boldsymbol{x}_2\rangle\langle \boldsymbol{x}_2|\Sigma(E)\,|\boldsymbol{x}_1\rangle\langle \boldsymbol{x}_1|p\rangle. \quad (93)$$

Defining the r.h.s. as a modified orbital, $\langle \boldsymbol{x}|p^*\rangle$, we have

$$\langle \boldsymbol{x}|p^*\rangle = \langle \boldsymbol{x}|p\rangle + \frac{\langle \boldsymbol{x}|i\rangle\langle i|\boldsymbol{x}_2\rangle\,\langle \boldsymbol{x}_2|\Sigma(E)|\boldsymbol{x}_1\rangle\,\langle \boldsymbol{x}_1|p\rangle}{E-\varepsilon_i+\mathrm{i}\gamma_i}. \quad (94)$$

But this is identical to the first expression (65) for the Brueckner orbital, if we replace ε_p^* by E. ***Therefore, the modified orbital*** (94) ***is identical to the Brueckner orbital or the Dyson orbital for the valence electron***. It follows from the identity (65) that this orbital can also be expressed

$$\langle \boldsymbol{x}|p^*\rangle = \langle \boldsymbol{x}|p\rangle + \frac{\langle \boldsymbol{x}|i\rangle\langle i|\boldsymbol{x}_2\rangle\,\langle \boldsymbol{x}_2|\Sigma^*(E)|\boldsymbol{x}_1\rangle\,\langle \boldsymbol{x}_1|p^*\rangle}{E-\varepsilon_i+\mathrm{i}\gamma_i}, \quad (95)$$

and it satisfies the same Dyson equation (67)

$$h_0\,\langle \boldsymbol{x}|p^*\rangle + \langle \boldsymbol{x}|\Sigma^*(E)|\boldsymbol{x}_1\rangle\langle \boldsymbol{x}_1|p^*\rangle = E\,\langle \boldsymbol{x}|p^*\rangle. \quad (96)$$

This demonstrates that the all-order perturbative (or coupled-cluster) approach and the Green's-function approach are completely equivalent in treating a single electron outside a closed-shell system – or a single hole in such a system.

4.5. Application to the affinity of the calcium atom

As an illustration of the Green's-function technique, we consider the calculation of the electron affinity of the Ca atom (see Table II). This is a very delicate quantity, which has resisted accurate experimental as well as theoretical determinations for a long time. For the negative Ca ion, the Hartree-Fock model does not even yield a bound state for the last electron.

The first experimental observation of the negative Ca ion in the $4p$ state was made by Pegg at al. in 1987 [37], and the affinity was measured to be 43± 7 meV. The first theoretical evaluation was made shortly afterwards by Froese-Fischer [17], who found a consistent value of the affinity, or 45 meV. Several subsequent calculations yielded values

Table II. Electron affinity of Ca atom (in meV)

	$4p_{1/2}$	$4p_{3/2}$	Reference
Theory	-19	-13	[40]
Theory	-22	-18	[1]
Expt'l	-24.55	-19.73	[38]
Expt'l	-18.4		[43]
Expt'l	-17.5		[34]

in the range 45-82 meV [40]. Later, the affinity was experimentally determined to be only about 18 meV [43, 34], and more recently the most accurate determination was performed by the Aarhus group with the result of 24.5 meV [38] for the ground state and about 20 meV for the first excited state.

In 1996 we performed an extensive high-order nonrelativistic Green's-function calculation of the affinities of Ca in the two lowest states, with the result of 19 and 13 meV, respectively. Shortly afterwards, Avgoustoglou and Beck performed a relativistic Green's-function calculation, limited to second order, which yielded the values 22 and 18 meV, respectively [1], in excellent agreement with the Aarhus results. Similar results have been obtained also for the negative Sr ion [1, 40]. These results show that the Green's-function method is quite a powerful technique that can be successfully applied also to intricate system like the negative alkaline-earth ions.

5. Summary and Conclusion

We have demonstrated that Brueckner and Dyson orbitals are identical concepts for a system with a single valence electron outside closed shells or with a single electron hole in a closed-shell system. It is also shown that the orbital energy eigenvalue corresponds to the exact electron binding energy or affinity, including all kinds of many-body effects. This conclusion is supported by numerical results. Both techniques are capable of yielding high-accuracy results also for highly correlated systems. The results shown for a single valence electron or a single valence hole can be extended to more general system, as will be demonstrated in a forthcoming publication.

Acknowledgments

I have benefitted a great deal from my contacts with Per-Olov Löwdin, who long ago introduced me to the fields of perturbation theory and many-body physics, particularly at an early Sanibel symposium and the associated winter school. My continuous contacts and discussions with Per Olov over the years have always been very stimulating and valuable for me and my work. I also want to express my gratitude to my coworker Sten Salomonson as well as to Rod Bartlett and Vincent Ortiz for stimulating discussion and correspondence.

References

1. Avgoustoglou, E. N. and D. R. Beck: 1997, '*All-order relativistic many-body calculations for the electron affinities of Ca^-, Sr^-, Ba^-, and Yb^- negative ions*'. *Phys. Rev. A* **5**5, 4143–49.
2. Bartlett, R. J. and G. D. Purvis: 1978, '*Many-Body Perturbation Theory, Coupled-Pair Many-Electron Theory, and the Importance of Quadruple Excitations for the Correlation Problem*'. *Int. J. Quantum Chem.* **1**4, 561–81.
3. Bloch, C.: 1958a, '*Sur la détermination de l'etat fondamental d'un système de particules*'. *Nucl. Phys.* **7**, 451–58.
4. Bloch, C.: 1958b, '*Sur la théorie des perurbations des etats liés*'. *Nucl. Phys.* **6**, 329–47.
5. Blundell, S. A., W. R. Johnson, Z. W. Liu, and J. Sapirstein: 1989, '*Relativistic all-order calculations of energies and matrix elements for Li and Be^+*'. *Phys. Rev. A* **4**0, 2233–46.
6. Brandow, B. H.: 1967, '*Linked-Cluster Expansions for the Nuclear Many-Body Problem*'. *Rev. Mod. Phys.* **3**9, 771–828.
7. Brenig, W.: 1957, '*Zweiteilchennäherungen des Mehrkörperproblems I*'. *Nucl. Phys.* **4**, 363–74.
8. Chernysheva, L. V., G. F. Gribakin, V. K. Ivanov, and M. Y. Kuchiev: 1988, '*Many-body calculation of negative ions using the Dyson equation*'. *J. Phys. B* **2**1, L419–25.
9. Chong, D. P., P. Aplincourt, and C. Bureau: 2002, '*Calculation of Core-Electron Binding Energies of Peptide Bond*'. *J. Phys. Chem. A* **1**06, 356–62.
10. Čižek, J.: 1966, '*On the Correlation Problem in Atomic and Molecular Systems. Calculations of Wavefunction Components in the Ursell-Type Expansion Using Quantum-Field Theoretical Methods*'. *J. Chem. Phys.* **4**5, 4256–66.
11. Coster, F. and H. Kümmel: 1960, '*Short-range correlations in nuclear wave functions*'. *Nucl. Phys.* **1**7, 477–85.
12. Coster, F.: 1958, '*Bound states of a many-particle system*'. *Nucl. Phys.* **7**, 421–24.
13. Dubza, V. A., V. V. Flambaum, P. G. Silvestrov, and O. P. Shuskov: 1985, ''. *J. Phys. B* **1**8, 597–613.
14. Eliaev, E., U. Kaldor, and Y. Ishikawa: 1994, '*Ionization potentials and excitation energies of the alkali-metal atoms by the relativistic coupled-cluster method*'. *Phys. Rev. A* **5**0, 1121–28.

15. Ey, W.: 1978, '*Degenerate many fermion theory in exp S form (III). Linked valence expansions*'. *Nucl. Phys. A* **2**96, 189–204.
16. Fetter, A. L. and J. D. Walecka: 1971, *The Quantum Mechanics of Many-Body Systems*. N.Y.: McGraw-Hill.
17. Froese-Fischer, C.: 1989, '*Binding energies for p electrons in negative alkaline-earth elements*'. *Phys. Rev. A* **3**9, 963–70.
18. Hubbard, J.: 1957, '*The description of collective motions in terms of many-body perturbation theory*'. *Proc. R. Soc. London, Ser. A* **2**40, 539–60.
19. Johnson, W. R., S. A. Blundell, and J. Sapirstein: 1988, '*Many-body perturbation theory calculations of energy levels along the lithium isoelectronic sequence*'. *Phys. Rev. A* **3**7, 2764–77.
20. Johnson, W. R., J. Sapirstein, and S. A. Blundell: 1989, '*Many-body theory applied to negative ions*'. *J. Phys. B* **2**2, 2341–47.
21. Koopmans, T.: 1933, '*Über die Zuordnung von Wellenfunktionen und Eigenwerten zu den einzelnen Elektronen eines Atoms*'. *Physica* **1**, 104–13.
22. Kümmel, H., K. H. Lührman, and J. G. Zabolitsky: 1978, '*Many-fermion theory in exp S (or coupled cluster) form*'. *Phys. Rep.* **3**6, 1–135.
23. Kvasnička, V.: 1974, ''. *Czech. J. Phys. B* **2**4, 605.
24. Linderberg, J. and Y. Öhrn: 1973, *Propagators in Quantum Chemistry*. London and New York: Academic Press.
25. Lindgren, I., J. Lindgren, and A.-M. Mårtensson: 1976, '*Many-Body Calculations of the Hyperfine Interaction of Some Excited States of Alkali Atoms, Using Approximate Brueckner or Natural Orbitals*'. *Z. Phys. A* **2**79, 113–25.
26. Lindgren, I. and J. Morrison: 1986, *Atomic Many-Body Theory*. Berlin: Second edition, Springer-Verlag.
27. Lindgren, I. and D. Mukherjee: 1987, '*On the connectivity criteria in the open-shell coupled-cluster theory for the general model spaces*'. *Phys. Rep.* **1**51, 93–127.
28. Lindgren, I. and S. Salomonson: 2002, '*Bruechner orbitals and density-functional theory*'. *Int. J. Quantum Chem.* **9**0, 294–308.
29. Lindgren, I.: 1974, '*The Rayleigh-Schrödinger perturbation and the linked-diagram theorem for a multi-configurational model space*'. *J. Phys. B* **7**, 2441–70.
30. Lindgren, I.: 1978, '*A Coupled-Cluster Approach to the Many-Body Perturbation Theory for Open-Shell Systems.*'. *Int. J. Quantum Chem.* **S**12, 33–58.
31. Lindgren, I.: 1985, '*Accurate many-body calculations on the lowest* ^2S *and* ^2P *states of the lithium atom*'. *Phys. Rev. A* **3**1, 1273–86.
32. Löwdin, P.-O.: 1962, '*Studies in Perturbation Theory. V. Some Aspects on the Exact Self-Consistent Field Theory*'. *J. Math. Phys.* **3**, 1171–84.
33. Migdal, A. B.: 1967, *Theory of Finite Fermi Systems and Applications to Atomic Nuclei*. N.Y., London, Sidney: Interscience, Wiley.
34. Nadeau, M.-J., X.-L. Zhao, M. A. Garvin, and A. E. Litherland: 1992, '*Ca negative-ion binding energy*'. *Phys. Rev. A* **4**6, R3588–90.
35. Ortiz, J. V.: 1999, '*Towards an exact one-electron picture of chemical bonding*'. *Adv. Quantum Chem.* **3**5, 33–52.
36. Paldus, J. and J. Čižek: 1975, '*Time-Independent Diagrammatic Approach to Perturbation Theory of Fermion Systems*'. *Adv. Quantum Chem.* **9**, 105–197.
37. Pegg, D., J. Thompson, R. Compton, and G. Alton: 1987, '*Evidence for a stable negative of calcium*'. *Phys. Rev. Lett.* **5**9, 2267–70.

38. Petrunin, V. V., H. H. Andersen, P. Balling, and T. Andersen: 1996, '*Structural properties of the negative calcium ion: Binding energies and fine-structure splitting*'. *Phys. Rev. Lett.* **7**6, 744–47.
39. Pople, J. A., R. Krishnan, H. B. Schlegel, and J. S. Binkley: 1978, '*Electron Correlation Theories and Their Application to the Study of Simple Reaction Potential Surfaces*'. *Int. J. Quantum Chem.* **1**4, 545–60.
40. Salomonson, S., H. Warston, and I. Lindgren: 1996, '*Many-Body Calculations of the Electron Affinity for Ca and Sr*'. *Phys. Rev. Lett.* **7**6, 3092–95.
41. Salomonson, S. and A. Ynnerman: 1991, '*Coupled-cluster calculations of matrix elements and ionization energies of low-lying states of sodium*'. *Phys. Rev. A* **4**3, 88–94.
42. Triguero, L., O. Plashkevych, L. G. M. Pettersson, and H. Ågren: 1999, '*Simple method for constructing accurate atomic Kohn-Sham potentials*'. *J. El. Spect. Rel. Phen.* **1**84, 195.
43. Walter, C. and J. Peterson: 1992, '*Shape resonance in Ca^- photodetachment and the electron affinity of $Ca(^1S)$*'. *Phys. Rev. Lett.* **6**8, 2281–84.
44. Wick, C. G.: 1950, '*The Evaluation of the Collision Matrix*'. *Phys. Rev.* **8**0, 268–272.